



Biological modelling / Biomodélisation

# On phytoplankton aggregation: a view from an IBM approach

Nadjia El Saadi <sup>a,\*</sup>, Alassane Bah <sup>a,b</sup>

<sup>a</sup> *Geodes-IRD, 32, avenue Henri-Varagnat, 93143 Bondy cedex, France*

<sup>b</sup> *ESP, Department of Computing, University Cheikh Anta Diop, Dakar, Senegal*

Received 22 March 2005; accepted after revision 2 May 2006

Available online 11 July 2006

Presented by Pierre Auger

## Abstract

In this paper, we build up an individual-based model (IBM) that describes the aggregative behavior in phytoplankton. The processes in play at the individual level (an individual = a phytoplankton cell) are: a random dispersal, a displacement due to the net effect of cells present in a suitable neighborhood (spatial interactions) and a branching (cell division and death). The IBM model provides a virtual world where phytoplankton cells appear to form clusters. Using this model, we explore the spatial structure of phytoplankton and present some numerical simulations that help the understanding of the aggregation phenomenon. **To cite this article:** *N. El Saadi, A. Bah, C. R. Biologies 329 (2006).*

© 2006 Académie des sciences. Published by Elsevier SAS. All rights reserved.

**Keywords:** IBM; Phytoplankton aggregation; Lagrangian model; Eulerian model; Clark–Evans Index

## 1. Introduction

Phytoplankton is a generic name for photosynthesizing microscopic organisms that inhabit the upper sunlit layer (euphotic zone) of almost all oceans and bodies of freshwater. They are agents for ‘primary production’ and the incorporation of carbon from the environment into living organisms, a process that sustains the aquatic food web [1].

More recent work has demonstrated the existence and potential importance of the formation of larger phytoplankton particles by aggregation [2–4]. However, the mechanisms governing aggregate formation have been poorly understood.

There has been extensive application of coagulation theory to describe aggregation of marine particles [5] and specifically phytoplankton aggregation [6,7]. Aggregation by physical coagulation requires that primary particles collide by some physical processes and stick together upon collision. Brownian motion, differences in sinking velocities and fluid shear may all cause primary particles to collide.

However, studies of marine aggregates at small scales have emphasized the biological mechanisms of their formation. That is, although planktonic organisms can be thought of as particles, the richness of biological responses makes the nature of their interactions more complex than the simple physical ones described by coagulation theory. Indeed, some planktonic species (algae, bacteria and dinoflagellates that are motile species of phytoplankton) have chemosensory abilities [8–10], that is, they can sense the chemical field generated by

\* Corresponding author.

*E-mail address:* [elsaadi@bondy.ird.fr](mailto:elsaadi@bondy.ird.fr) (N. El Saadi).

the presence of other cells. The dinoflagellates and more generally motile algae are known to leak organic matter such as amino-acids and sugar into solution [11] and this leakage creates zones around individual cells called ‘phycospheres’, where extracellular products exist in enhanced concentrations over the background [12]. The chemosensory responses allow dinoflagellates and algae that are present in a suitable neighborhood to find the leaky cells and to stay near them, forming aggregates. There has been no quantitative study of the nature of chemosensory interactions between dinoflagellates, even although chemosensory behavior in dinoflagellates may have importance in their search for food and for chemical defense [8–10,13–15]. Indeed, recent studies of micro-organisms have revealed diverse complex social behavior in dinoflagellates, such as cooperation in foraging and defense [9,16,17]. For instance, *Pfiesteria* dinoflagellates act as ambush predators, synchronously releasing toxins to kill all fish over many square kilometres, after which the dinoflagellates feed on the carcasses. On an other hand, many studies suggest that there will be a density at which dinoflagellates metabolites (for instance, an altruist production of toxins DMS (dimethyl sulfide)) will inhibit grazing and provide a protective feedback loop.

Based on the ideas of small scale biological mechanisms for aggregates formation, El Saadi and Arino [18,19] have investigated a Lagrangian model which provides an explanation of the aggregation behavior in phytoplankton in terms of attraction mechanisms among cells due to the chemosensory behavior, random branching (birth and death), in addition to individual random dispersals described by independent Brownian motions. The aim of such modelling was to catch the main features of the individual dynamics at small scales which are responsible at a larger scale for a more complex behavior that leads to the formation of aggregating patterns. An Eulerian description has been rigorously derived as a continuum limit [18,19] by using the approach in [20] based on martingale properties of a sequence of approximating interacting branching-diffusion processes. The Eulerian model of phytoplankton aggregation is described by the following nonlinear stochastic partial differential equation defined in space of vector measures:

$$dY_t = D\Delta Y_t dt - \nabla \cdot [Y_t(F_a * Y_t)] dt + dM_t \quad (1)$$

where  $Y_t$  is a measure describing the spatial distribution of phytoplankton cells at time  $t$ . The diffusion term in (1) takes into account the spatial spread of the phytoplankton cells with the coefficient of diffusion  $D$ ,

while the advection term describes the interaction mechanisms among particles via the velocity  $F_a * Y_t$ . The latter has the form of convolution [21–23], with  $F_a$  the attractive force.  $M_t$  is a continuous orthogonal martingale measure with covariance measure  $\mu Y_s(dx) ds$  (in the sense of Walsh [24]), where  $\mu$  is the rate of branching. We can think of  $M_t$  as white noise (in the sense of Walsh) representing the random imbalance between births and deaths due to space, that is, binary division puts always parent and progeny at the same position while death occurs anywhere. This asymmetry is represented in the term  $M_t$ .

In [25], it has been shown that if the branching phenomenon is not present in the phytoplankton story,  $Y_t$  (for every  $t > 0$ ) is absolutely continuous with respect to the Lebesgue measure on  $\mathbb{R}$ , and hence, admits a density  $f(t, x)$  which satisfies the integro-differential advection–diffusion equation:

$$\frac{\partial f(t, x)}{\partial t} = D \frac{\partial^2}{\partial x^2} f(t, x) - \frac{\partial}{\partial x} [f(t, x)(F_a * f(t, \cdot))(x)]. \quad (2)$$

This equation has been analyzed mathematically in [25] and furthermore, authors have proved the existence of nonuniform stationary solutions. The biological significance of this asymptotic result is that nonlinear interactions between phytoplankton cells at small scales can produce aggregating patterns in water at large scales.

This paper is a contribution in exploring phytoplankton aggregation behaviors using an IBM approach. The IBM’s models have known an important development in the 1990s stimulated by the availability of powerful personal computers [26–28]. The article written by Huston et al. [29] is the most frequently quoted. These authors argue that the development of this approach is due to the need to take into account the individual because of his genetic uniqueness and, secondly, the fact that each individual is situated and his interactions are local. We recall that the principle of an IBM consists in following each individual of a collection, assuming they move or some of their characteristics change during a time step, due to a number of influences such as individual behavior, interactions of individuals with one another, interactions of individuals with a resource distribution [30]. So in this work, we propose to build a numerical IBM (Individual-Based Model) version arising from the Lagrangian model of phytoplankton in [18,19] and present the simulations results showing the behavior of the system of stochastic differential equations in [18,19]. Our goal is twofold: first, to visualize the formation of clusters, and second, to measure and compare influences of

the different processes involved at the cell level on appearing of aggregation patterns.

The paper is organized as follows: in Section 2, we describe the Lagrangian aggregation model of phytoplankton built in [18,19]. Section 3 is devoted to the simulator description and in Section 4, we present the different scenarios to be tested. Section 5 summarizes the simulations results. These correspond to the following issues: (1) the Clark–Evans Index; (2) the spatial and temporal distribution of phytoplankton cells; (3) the effect of diffusion; and (4) the effect of perception. Section 5 offers a discussion of the results and finally, we give some conclusions in Section 6.

## 2. Lagrangian aggregation model

We recall that the Lagrangian model of phytoplankton aggregation in [18,19] is built up as follows:

### 2.1. Spatial motion

We consider  $N$  phytoplankton cells ( $N$  is a positive integer), each of them having at some time a certain position. Let  $(X_N^i(t))_{1 \leq i \leq N}$  be the family of positions for the  $N$  cells.

The spatial motion of phytoplankton cells is described via the following system of stochastic differential equations:

$$dX_N^i(t) = F[(X_N^l(t))_{1 \leq l \leq N}](X_N^i(t)) dt + \sqrt{2D} dB_i(t) \quad i = 1, \dots, N \quad (3)$$

where  $(B_i(t))$ ,  $i = 1, \dots, N$ , are independent Brownian motions. The dispersion term expresses the diffusion of phytoplankton cells in water, which is similar to molecular diffusion [31,32] and  $D$  is the diffusion coefficient. The drift term  $F$  in (3) describes the interactions between the  $i$ th cell and the other cells in the system.

### 2.2. Spatial interactions

To describe interactions between phytoplankton particles, we propose the ideas involving non-uniformity of the concentration fields around organisms and consider phytoplankton cells having chemosensory abilities (dinoflagellates, algae) and hence some knowledge about their neighbors. However, each cell has a limited knowledge of the spatial distribution of its neighbors because it cannot detect small concentration differences over its length [31,33,34].

Taking into account these biological considerations, we assume that aggregation forces act over a specific

range of sensitivity and thus we model pair interactions as follows:

- The presence of a cell in position  $y$  induces on a cell in position  $x$  an attractive force that depends on the distance between the two cells and which is determined by:

$$K(x, y) = \frac{1}{N} F_a(x - y) \quad (4)$$

where

$$F_a(z) = -\frac{z}{\|z\|} (-\|z\|^2 + (r_0 + r_1)\|z\| - r_0r_1) \times 1_{]r_0, r_1[}(\|z\|) \quad (5)$$

( $r_0$  and  $r_1$  are the non negative reals that delimit the range of sensitivity in phytoplankton).

The normalization factor  $1/N$  in (4) corresponds to associating the mass  $1/N$  to each phytoplankton cell [23,35].  $F_a(x - y)$  leads to the attraction of the cell in position  $x$  to that in  $y$ . The quantity  $(-\|x - y\|^2 + (r_0 + r_1)\|x - y\| - r_0r_1)$  gives the magnitude of  $F_a(x - y)$  as a function of the distance  $\|x - y\|$ . The direction of  $F_a(x - y)$  is given by the unitary director vector  $-(x - y)/(\|x - y\|)$ . The cell in position  $x$  is not attracted to that in  $y$  if  $\|x - y\| \leq r_0$ , because in the closest vicinity of  $y$  is the largest concentration of the substances released by the cell in  $y$ . It has been reported that large concentrations of products such as amino acids, organic compounds and sugar inhibit the chemosensory behavior in dinoflagellates and motile algae [8];

- The drift  $F[(X_N^l(t))_{1 \leq l \leq N}](X_N^i(t))$  is the superposition of all cells effects of the system on the  $i$ th cell. It is given by:

$$F[(X_N^l(t))_{1 \leq l \leq N}](X_N^i(t)) = \sum_{j=1, j \neq i}^N K(X_N^i(t), X_N^j(t)).$$

### 2.3. Branching

The cells branch. The most common mean of reproduction in phytoplankton is asexual cell division (mitosis). This process splits the organism into two identical copies. So, we assume that each cell can die, divide into two or remain unchanged with equal probabilities. If the phytoplankton cell splits, the two new cells begin their life at the branching point. They move following Eq. (3) until the time they themselves branch and so on. A cell division can occur once every day.

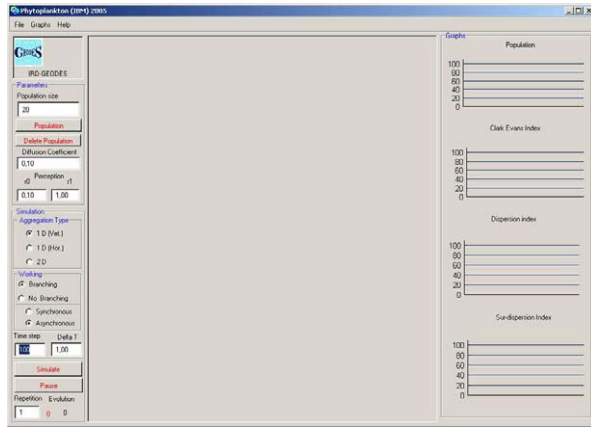


Fig. 1. The interface of the simulator.

### 3. The simulator

We now present the IBM arising from the Lagrangian model introduced in the previous section, that is its computer simulation model.

The simulator we conceived is a tool of experiments intended to represent virtually individual aggregating behavior. It is implemented in the object-oriented language Smalltalk using the Visual Works Environment. The model of this simulator is based on the discrete version of the system of stochastic differential equations (3) with  $K$  replaced by (4). Time evolves in a discrete way by steps  $\Delta t$ . The initial condition ( $t = 0$ ) is prepared by placing randomly and independently  $N$  particles. Each time step consists of two stages: (1) branching (random birth and death); (2) spatial motion. At the first stage, each particle splits into two or dies or remains unchanged with equal probabilities. If it splits, the new particle is placed on top of the parent; if it dies, it is removed from the system. In stage 2, the  $i$ th particle is displaced to a new position:

$$X_i(t + \Delta t) = X_i(t) + \frac{1}{N(t)} \sum_{j=1, j \neq i}^{N(t)} F_a(X_i(t) - X_j(t)) \Delta t + \Theta_i \sqrt{2D \Delta t}$$

where  $N(t)$  is the population size at time  $t$  and  $(\Theta_i)_{1 \leq i \leq N(t)}$  are independent and identically distributed Standard Gaussian random variables.

The simulator is provided with an interface to perform action-to-visualize the aggregation behavior (Fig. 1). It consists on three components:

- (i) the parameter window (on the left) that allows the user the set up of the global variables;

- (ii) the situation window (at the center of the interface) that represents positions of individuals;
- (iii) the indicator window (on the right) that allows to visualize evolution of different indicators of aggregation.

The simulator offers the possibility of visualizing the dynamics of phytoplankton cells in 1D (vertically or horizontally) and in 2D. It permits one to undertake simulations in two situations: the model including branching mechanisms (model I) and the model without branching (model II) (that is, the population size remains fixed). It has also been performed in order to quantify the evolution of different indicators of aggregation (Clark–Evans Index, the dispersion index and the surdispersion index) [36]. The last analyzes and characterizes the spatial structure of the particle pictures shown by the simulator.

For a purely qualitative aim, we present some particle pictures describing the reproduction and temporal-spatial spread of phytoplankton communities in 1D (Fig. 2) and 2D (Fig. 3).

In this work, we restrict ourselves to the 1D numerical results obtained by using the Clark–Evans Index defined as:

$$CEI = \frac{\bar{r}_A}{\bar{r}_E}$$

where  $\bar{r}_A = (\sum_{i=1}^N r_i) / N$  is the mean of the distances to the nearest neighbor ( $r_i$  is the distance in any specified units from individual  $i$  to its nearest neighbor) and  $\bar{r}_E$  is the mean distance to nearest neighbor expected in an infinitely large random distribution of density  $\lambda$ .

It has been shown (see [37]) that:

$$\bar{r}_E = \frac{1}{\lambda} \quad \text{in 1D}$$

and

$$\bar{r}_E = \frac{1}{2\sqrt{\lambda}} \quad \text{in 2D.}$$

The density  $\lambda$  is expressed as the number of individuals per unit area. The unit of measurement used in the calculation of  $\lambda$  must be the same as that used in measuring the  $r_i$  ( $i = 1, \dots, N$ ). The ratio of the observed mean distance  $\bar{r}_A$  to the expected mean distance serves as the measure of departure from randomness. The use of this indicator is very simple. It gives a very simplistic view of the spatial structure, namely,  $CEI = 1$  if the spatial structure is random,  $CEI > 1$  if the spatial structure is regular and  $CEI < 1$  if it is aggregated. Under conditions of maximum aggregation,  $CEI = 0$  since all of

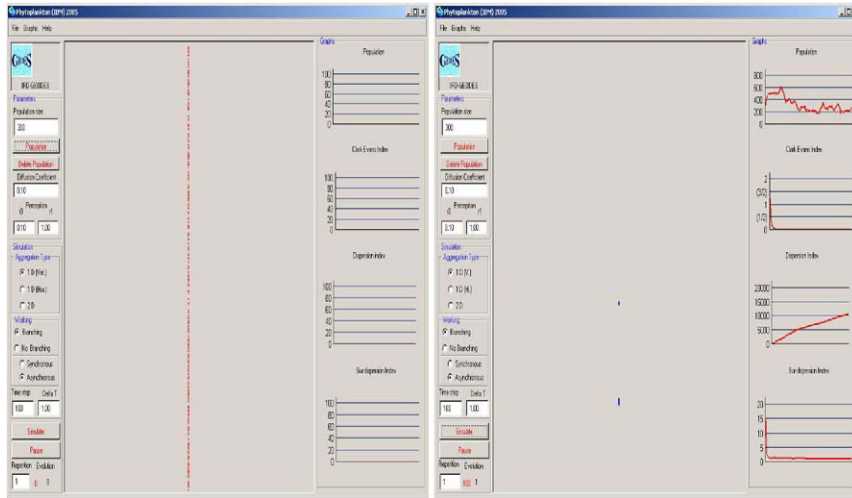


Fig. 2. A time-evolution result for the Lagrangian model in 1D.

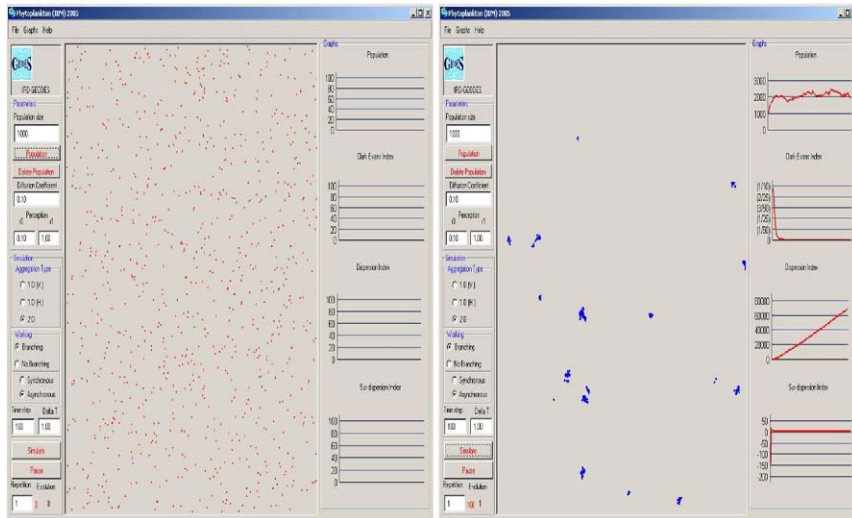


Fig. 3. A time-evolution result for the Lagrangian model in 2D.

the individuals occupy the same locus and the distance to nearest neighbor is therefore 0.

Our approach in using this indicator has a double goal: on the one hand, we intend to explore the spatial structure of the particle pictures stemmed from both model I and model II, and on the other hand, to measure and compare influences of the different processes in play (random dispersion, chemosensory interactions and branching) on the aggregating patterns.

#### 4. Scenarios tested

The Lagrangian model in Section 2 gives an explanation of the phytoplankton aggregating behavior in terms of a diffusion with velocity  $D$ , attractive forces acting in

a perception zone delimited by  $r_0$  and  $r_1$  and a branching with a fixed rate.

We are therefore going to explore several scenarios corresponding to different values of  $D$  and  $r_1$ . The values of  $D$  are chosen to correspond at three different orders of magnitude that cover possible values of phytoplankton diffusion quoted in the literature. These values are ( $D = 0.001 \mu\text{m}^2/\text{s}$ ,  $0.01 \mu\text{m}^2/\text{s}$ ,  $0.1 \mu\text{m}^2/\text{s}$ ). For  $r_1$ , we consider different arbitrary possible values that are well suited to the choice of  $r_0$  ( $r_1 = 1, 10, 20 \mu\text{m}$ ). We fixed  $r_0 = 0.1 \mu\text{m}$  an arbitrary value chosen very small in comparison to the values of  $r_1$  ( $r_0 \ll r_1$ ) [30].

Although many preliminary experiments have shown no variability in the outputs, we perform five runs of the

Table 1  
Table of scenarios

$D \setminus r_1$	1 ( $\mu\text{m}^2$ )	10 ( $\mu\text{m}^2$ )	20 ( $\mu\text{m}^2$ )
0.001 ( $\mu\text{m}^2/\text{s}$ )	S1	S2	S3
0.01 ( $\mu\text{m}^2/\text{s}$ )	S4	S5	S6
0.1 ( $\mu\text{m}^2/\text{s}$ )	S7	S8	S9

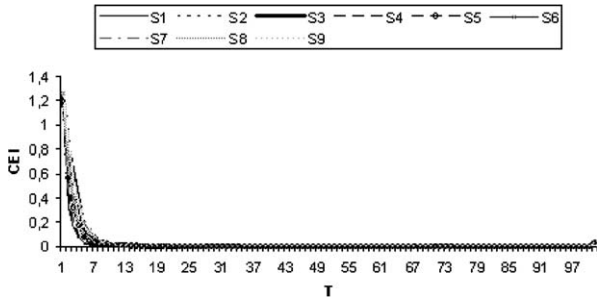


Fig. 4. The CEI's evolution in time for model I.

simulation for each scenario to damp out any randomness embodied in the simulator. Hence, each simulation result presented in the next section is an average of five repetitions. Furthermore, these preliminary experiments have also shown that  $T = 1000\Delta t$  for model II and  $T = 100\Delta t$  for model I are sufficient long time to reach stable aggregative structures, with a time step  $\Delta t = 1$  s. To connect these simulations with reality, we let  $\Delta t$  correspond to 1 day in reality, since a cell division holds once every day.

The nine scenarios summarized in Table 1 are explored in the two cases:

- (1) model I (the interacting branching model);
- (2) model II (the interacting model without branching).

**5. Simulations results**

We present the simulations results obtained for an initial population size  $N = 300$ , with a random initial distribution. A difference appears between results coming from models I and II. Moreover, in the case of model II, some differences due to the variation of the parameters  $D$  and  $r_1$  are observed between the scenarios.

*5.1. Result 1 (Clark–Evans Index)*

A difference in the evolution of the Clark–Evans Index (CEI) between models I and II is shown in Figs. 4 and 5.

For model I, the CEI is close to 0 in all the scenarios, which indicates a strong aggregation. The values

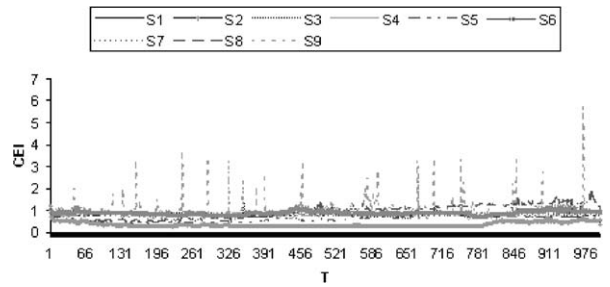


Fig. 5. The CEI's evolution in time for model II.

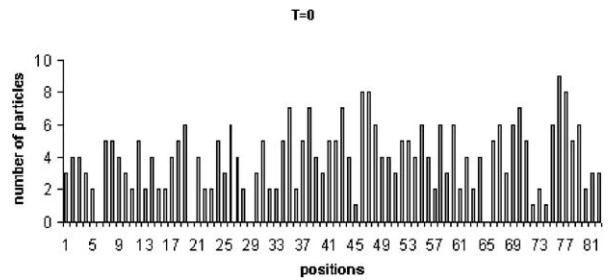


Fig. 6. The initial spatial distribution.

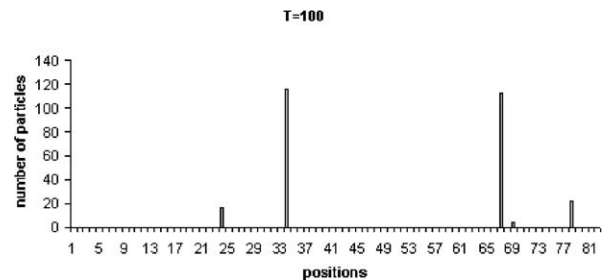


Fig. 7. The spatial distribution of model I at time  $T = 100$ .

greater than 0 observed earlier the date  $T = 7$  s are due to the randomness of the initial distribution. In the case of model II, the CEI is greater than 0 in all the scenarios, which corresponds to a less good aggregating behavior. The best aggregation in this case is observed in scenario 2, while instability is observed in scenario 9.

*5.2. Result 2 (spatial and temporal distribution)*

Both of models I and II in Figs. 7 and 8 show clusters formation from a random initial distribution (Fig. 6). Not only in the figure of model II, the clusters have larger diameter and small sizes, but also the peaks of the density profile observed in the figure of model I are higher: the aggregation phenomenon is stronger in the case of an interacting model with branching.

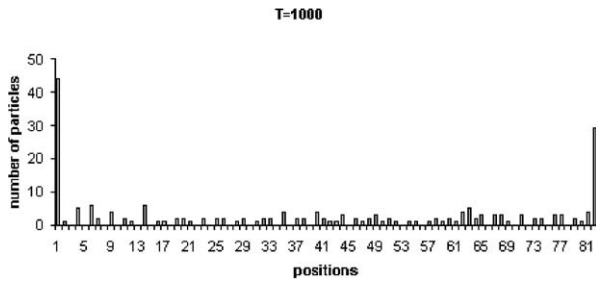


Fig. 8. The spatial distribution of model II at time  $T = 1000$ .

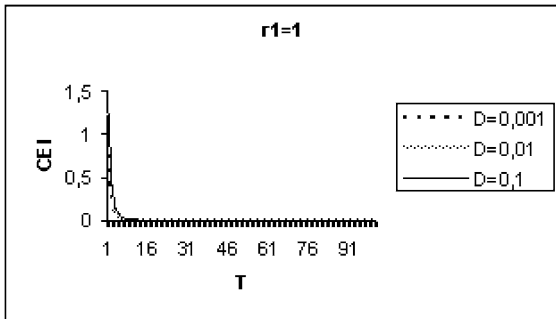


Fig. 9. The CEI variation in time when  $r_1 = 1$  (model I).

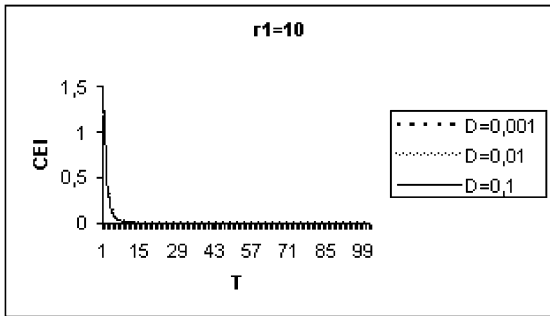


Fig. 10. The CEI variation in time when  $r_1 = 10$  (model I).

### 5.3. Result 3 (effect of diffusion)

Experiments in Figs. 9 to 11 show that for model I, the CEI is not affected by a variation of  $D$ . However, in the case of model II (Figs. 12 to 14), there are some differences in the evolution of the CEI. Aggregation is better for a weak diffusion coefficient and instability occurs for largest values of  $D$ .

### 5.4. Result 4 (effect of the perception zone)

As shown in Figs. 15 to 17, the CEI is not affected by a variation of the perception radius length, in the case of model I. For model II (Figs. 18 to 20), differences are observed in the CEI evolution. The best aggregation is

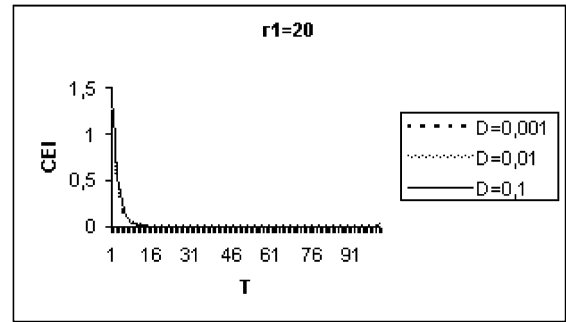


Fig. 11. The CEI variation in time when  $r_1 = 20$  (model I).

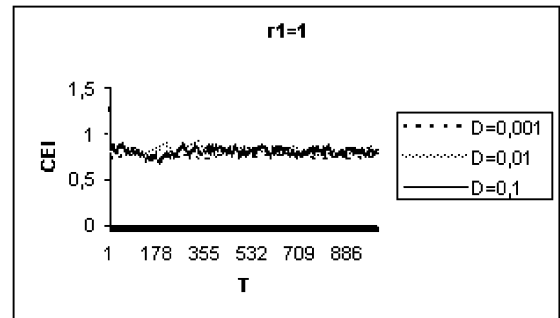


Fig. 12. The CEI variation in time when  $r_1 = 1$  (model II).

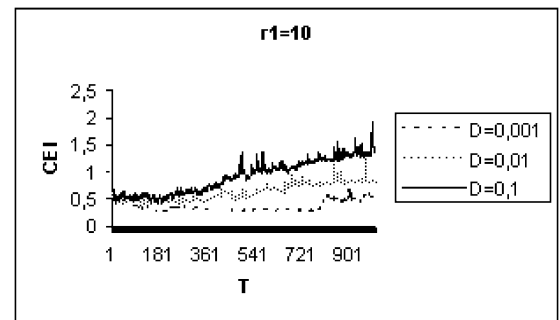


Fig. 13. The CEI variation in time when  $r_1 = 10$  (model II).

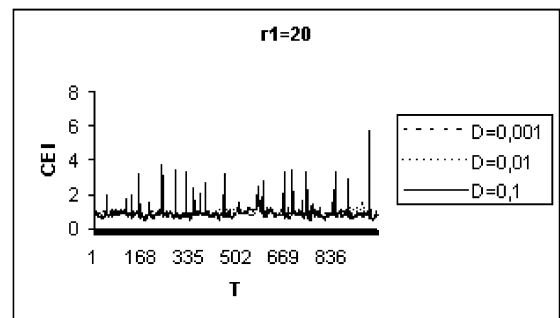


Fig. 14. The CEI variation in time when  $r_1 = 20$  (model II).

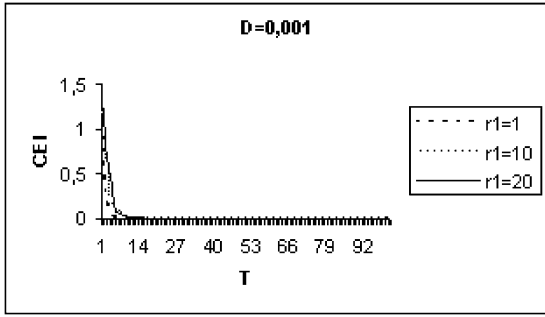


Fig. 15. The CEI variation in time when  $D = 0.001$  (model I).

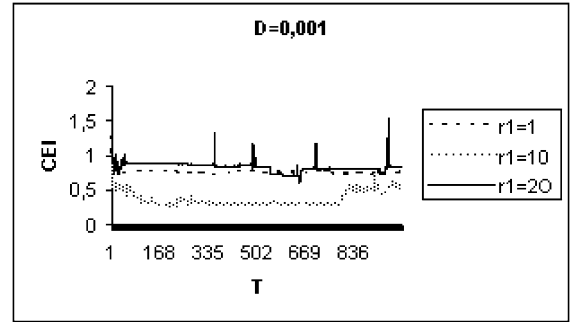


Fig. 18. The CEI variation in time when  $D = 0.001$  (model II).

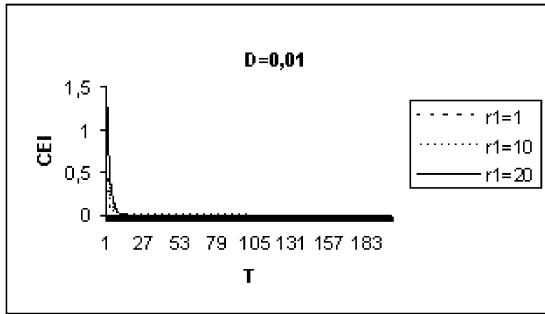


Fig. 16. The CEI variation in time when  $D = 0.01$  (model I).

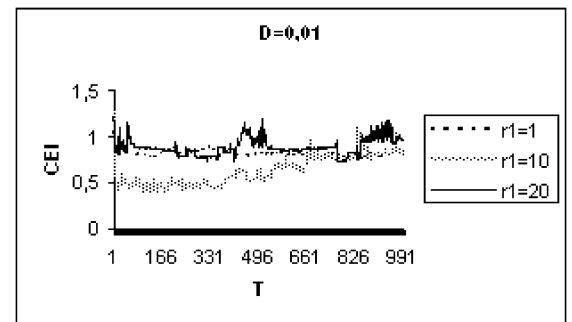


Fig. 19. The CEI variation in time when  $D = 0.01$  (model II).

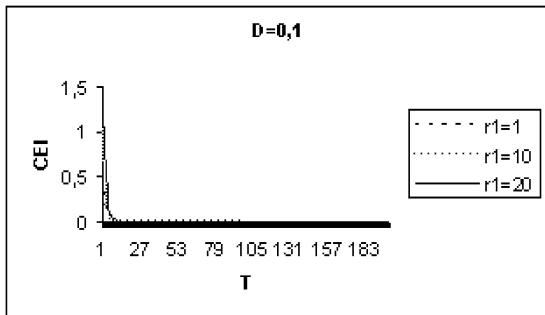


Fig. 17. The CEI variation in time when  $D = 0.1$  (model I).

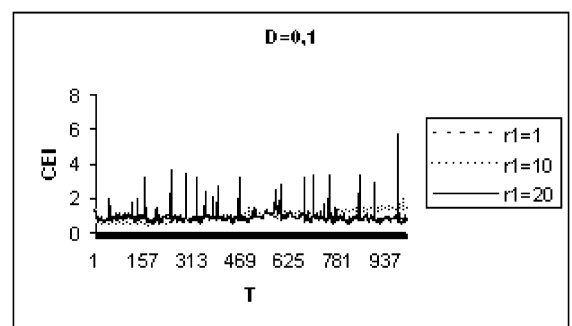


Fig. 20. The CEI variation in time when  $D = 0.1$  (model II).

observed for  $r_1 = 10$  and a great number of fluctuations appears at largest value of  $r_1$ .

**6. Discussion**

All the simulations results presented earlier make obvious the aggregating phenomenon in phytoplankton. Indeed, the CEI is always less than 1 in both of models I and II, that is, clusters do not form only when particles (phytoplankton cells) diffuse, interact spatially and branch, but even when the branching process is ignored. This last result confirms our asymptotic analytic result in [25] on the emergence of aggregating patterns at large

scale from a particle system with nonlinear interactions at small scales.

However, a difference is noticed between the interacting model with branching and that without branching. Aggregation is stronger and more visible when branching mechanisms are taken into account. From a biological view, this is due to the spatial aspects coupled to the branching mechanism. Indeed, there is a fundamental difference between the locations of birth and death: deaths occur anywhere but births always occur adjacent to living organisms. The accumulation of these small-scale density fluctuations produce the palpable nonuniformities detected in Figs. 2 and 3.

Diffusion and sensory distances have both a role on the aggregating behavior but this role remains negligible comparatively to the branching effect. It is clear this is due to the small values of the diffusion coefficient for phytoplankton ( $D < 1$ ) and to the different lengths of the perception radius chosen for  $r_1$ . Some simulations (which we do not present here) show that greater values of  $D$  and  $r_1$  (for example,  $D$  beyond 5 and  $r_1$  beyond 30) lead to particle pictures very different of those presented in this paper. Effects of the diffusion and/or the sensory distance on the quality of the aggregation behavior are better observed when branching mechanisms are ignored. In the latter, simulations show a transition from a random distribution to an organized structure with formation of weak clusters characterized by their larger radius and lower sizes, in contrast with the clusters occurring when branching; and the best situation for aggregation in this case is when diffusion is weak and the radius of perception is average. Instability in the spatial structure often occurs for the interacting model without branching. We think that this observation can give some intuitive insight on the stability of the steady-state solution in [25].

## 7. Conclusions

In this paper, an IBM approach was undertaken in the study of the aggregation process in phytoplankton. We have conceived and simulated the IBM discrete version corresponding to the mathematical Eulerian model in [18,19]. Simulations results show the formation of clusters, qualitatively by visualizing the aggregation phenomenon and quantitatively by using an aggregation indicator: the Clark–Evans Index.

The main result of this work is that branching has an eminent role in the phytoplankton aggregation process. We point out that Young in his paper [38], has shown that a population of independent random-walking organisms, reproducing by binary division and dying at constant rates, aggregates and clusters form out of spatially homogeneous initial condition without environmental variability, kinesis or taxis. He stressed the fact that the clustering mechanism can be driven only by reproduction and death (branching), provided the diffusion is not too strong relative to the reproduction rate. Here in this work, we rediscover Young's result of [38,39], although our population is spatially dependent. Indeed, simulations results stemmed from our IBM model have shown the formation of very weak clusters when only diffusion and interactions are involved in the model, while the clustering mechanism becomes more important and visible when branching

is taken into account. Consequently, the IBM approach presented in this paper, confirms that the mathematical Eulerian model (1) investigated in [18,19] is really an aggregation model and establishes the importance of branching on the aggregation phenomenon relative to nonlinear interactions and diffusion.

On another hand, many qualitative and quantitative results on the spatial distribution, sizes and positions of aggregates in space and time could be provided by our IBM model.

## Acknowledgements

The authors would like to thank Professors Pierre Auger, Jean-Pierre Treuil, Christian Mullon, and Nicolas Baccar for numerous useful discussions.

## References

- [1] S. Ghosal, M. Rogers, A. Wray, The turbulent life of phytoplankton, in: Proceedings of the Summer Program, Center for Turbulence Research, 2000.
- [2] G.A. Jackson, A model of the formation of marine algal flocks by physical coagulation processes, *Deep-Sea Res.* 37 (1990) 1197–1211.
- [3] U. Riebesel, D.A. Wolf-Gladrow, The relationship between physical aggregation of phytoplankton and particle flux: a numerical model, *Deep-Sea Res.* 1 39 (1992) 1085–1102.
- [4] P.S. Hill, Reconciling aggregation theory with observed vertical fluxes following phytoplankton blooms, *J. Geophys. Res.* 97 (1992) 2295–2308.
- [5] I.N. McCave, Size spectra and aggregation of suspended particles in the deep ocean, *Deep-Sea Res.* 31 (1984) 329–352.
- [6] G.A. Jackson, R. Maffione, D.K. Costello, A.L. Alldredge, B.E. Logan, H.G. Dam, Particle-size spectra between 1  $\mu\text{m}$  and 1 cm at Monterey Bay determined using multiple instruments, *Deep-Sea Res.* 1 44 (11) (1997) 1739–1767.
- [7] T. Kjørboe, Formation and fate of marine snow: small-scale processes with large-scale implications, *Sci. Mar.* 655 (suppl. 2) (2001) 57–71.
- [8] W.K. Fitt, Chemosensory responses of the symbiotic dinoflagellate *Symbiodinium microadriaticum* (Dinophyceae), *J. Phycol.* 21 (1985) 62–67.
- [9] H.J. Spero, M. Morée, Phagotrophic feeding and its importance to the life cycle of the holozoic dinoflagellate, *Gymnodinium fungiforme*, *J. Phycol.* 17 (1981) 43–51.
- [10] H.J. Spero, Chemosensory capabilities in the phagotrophic dinoflagellate *Gymnodinium Fungiforme*, *J. Phycol.* 21 (1985) 181–184.
- [11] T.H. Mague, E. Friberg, D.J. Hughes, I. Morris, Extracellular release of carbon by marine phytoplankton: a physiological approach, *Limnol. Oceanogr.* 25 (1980) 262–279.
- [12] W. Bell, R. Mitchell, Chemotactic and growth responses of marine bacteria to algal extracellular products, *Biol. Bull.* 143 (1972) 265–277.
- [13] D.C. Hauser, R.M. Levandowsky, S.H. Hunter, L. Chunosoff, J.S. Hollwitz, Chemosensory responses by the heterotrophic marine dinoflagellate *Cryptothecodinium cohnii*, *Microb. Ecol.* 1 (1975) 246–254.

- [14] M. Levandowsky, D.C.R. Hauser, Chemosensory responses of swimming algae and protozoa, *Int. Rev. Cytol.* 53 (1978) 145–210.
- [15] M. Levandowsky, Behaviour of dinoflagellates, in: F.J.R. Taylor (Ed.), *Biology of Dinoflagellates*, Blackwell Scientific Publications, Oxford, New York, 1985.
- [16] B.J. Crespi, The evolution of social behavior in microorganisms, *Trends Ecol. Evol.* 16 (4) (2001) 178–183.
- [17] G.V. Wolfe, The chemical defense ecology of marine unicellular plankton: constraints, mechanisms and impacts, *Biol. Bull.* 198 (2000) 225–244.
- [18] N. El Saadi, Modélisation et études mathématique et informatique de populations structurées par des variables aléatoires. Application à l'agrégation du phytoplancton, PhD thesis, Université de Pau et des pays de l'Adour, France, 2004.
- [19] N. El Saadi, O. Arino, A stochastic partial differential equation for phytoplankton aggregation, *Pacific Asian J. Math.*, Serial Publ., 2006, in press.
- [20] S. Méléard, S. Roelly, Interacting measure branching processes. Some bounds for the support, *Stochastics Stochastics Rep.* 44 (1993) 103–121.
- [21] A. Mogilner, L. Edelstein-Keshet, A nonlocal model for a swarm, *J. Math. Biol.* 38 (1999) 534–570.
- [22] S. Boi, V. Capasso, D. Morale, Modeling the aggregative behavior of ants of the species *Polyergus rufescens*, *Nonlinear Anal.: Real World Appl.* 1 (2000) 163–176.
- [23] D. Morale, V. Capasso, K. Oelschläger, An interacting particle system modelling aggregation behavior: from individuals to populations, *J. Math. Biol.* 50 (1) (2004) 49–66.
- [24] J.B. Walsh, An introduction to stochastic partial differential equations, *École d'été de probabilités de Saint-Flour*, Lecture Notes in Mathematics, vol. 1180, Springer-Verlag, 1986.
- [25] M. Adioui, O. Arino, N. El Saadi, A non local model of phytoplankton aggregation, *Nonlinear Anal.: Real World Appl.* 6 (2005) 593–607.
- [26] F. Bousquet, C. Lepage, Multi-agent simulations and ecosystem management: a review, *Ecol. Model.* 176 (2004) 313–332.
- [27] D.L. DeAngelis, L.J. Gross, *Individual-Based Models and Approaches in Ecology, Populations Communities and Ecosystems*, Routledge, Chapman and Hall, New York, 1992.
- [28] V. Grimm, Ten years of individual-based modelling in ecology: what have we learned and what could be learned in the future, *Ecol. Model.* 115 (1999) 129–148.
- [29] M. Huston, D.L. DeAngelis, W. Post, New computer models unify ecological theory, *Biosciences* 38 (1988) 682–691.
- [30] A. Mogilner, L. Edelstein-Keshet, L. Bent, A. Spiros, Mutual interactions, potentials and individual distance in a social aggregation, *J. Math. Biol.* 47 (2003) 353–389.
- [31] H.C. Berg, E.M. Purcell, Physics of chemoreception, *Biophys. J.* 20 (1977) 193–219.
- [32] P. Gros, La représentation de l'espace dans les modèles de dynamique de populations, IFREMER, Centre de Brest, France, 2001.
- [33] G.A. Jackson, Simulating chemosensory responses of marine microorganisms, *Limnol. Oceanogr.* 32 (6) (1987) 1253–1266.
- [34] G.A. Jackson, Simulation of bacterial attraction and adhesion to falling particles in an aquatic environment, *Limnol. Oceanogr.* 34 (3) (1989) 514–530.
- [35] D. Morale, Modeling and simulating animal grouping. Individual-based models, *Future-Generation Comput. Syst.* 17 (2001) 883–891.
- [36] F. Goreaud, P. Couteron, Les processus ponctuels, un outil pour décrire et modéliser la structure spatiale d'ensembles de points. Application aux peuplements forestiers, Cours ENGREF, France, 2003.
- [37] P.J. Clark, F.C. Evans, Distance to nearest neighbor as a measure of spatial relationships in populations, *Ecology* 35 (1954) 445–453.
- [38] W.R. Young, A.J. Roberts, G. Stuhne, Reproductive pair correlations and the clustering of organisms, *Nature* 412 (2001) 328–331.
- [39] W.R. Young, Brownian bugs and superprocesses, in: *Proc. 12th Aha Huliko'a Hawaiian Winter Workshop-Mixing*, 2001.